11th World Congress on Computational Mechanics (WCCM XI)
5th European Conference on Computational Mechanics (ECCM V)
6th European Conference on Computational Fluid Dynamics (ECFD VI)
E. Oñate, J. Oliver and A. Huerta (Eds)

# CHALLENGES FOR TIME AND FREQUENCY DOMAIN AEROACOUSTIC SOLVERS

**Aleksandar Angeloski[1,*], Marco Discacciati[1], César Legendre[2], Gregory Lielens[2] and Antonio Huerta[1]**

[1] Laboratori de Càlcul Numeric (LaCàN), Departament de Matematica Aplicada III
E.T.S. de Ingenieros de Caminos, Canales y Puertos,
Universitat Politecnica de Catalunya, BarcelonaTech, 08034 Barcelona, Spain.
e-mail: {aleksandar.angeloski,marco.discacciati,antonio.huerta}@upc.edu, web:
http://www.lacan.upc.edu/
[2] Free Field Technologies S.A.,
Mont-Saint-Guibert, 1435, Belgium
e-mail: {cesar.legendre,gregory.lielens}@fft.be, web http://www.fft.be/

**Key words:** aeroacoustics, linearized Euler equations, discontinuous Galerkin, noise prediction, propagation, time, frequency domain.

**Abstract.** The linearized Euler equations (LEE) model acoustic propagation in the presence of rotational mean flows. They can be solved in time [1–3] or in frequency [4–6] domain, with both approaches having advantages and disadvantages. Here, those pros and cons are detailed, both from a modeling and a numerical/computational perspective. Furthermore, a performance comparison and cross-validation between two frequency and time domain state-of-the-art solvers is performed. The frequency domain solutions are obtained with the hybridizable discontinuous Galerkin (HDG) [7–12] and the embedded discontinuous Galerkin (EDG) [13–15] method, while the time domain solver is an explicit discontinuous-Galerkin based solver [1]. The performance comparison and cross-validation is performed on a problem of industrial interest, namely acoustic propagation from a duct exhaust in the presence of realistic mean flow.

## 1 INTRODUCTION

Aeroacoustics is still a challenging application area both for computational models (either in time or frequency domains) and for numerical methods. Previous contributions [4–6] advocate for linearized Euler equations (LEE) in frequency domain. For instance, in [6] the authors select a continuous Galerkin (CG) approach rather than a discontinuous Galerkin (DG) method to reduce memory requirements. Whereas, in [5] DG is compared with a streamline upwind Petrov-Galerkin (SUPG) method and concludes that DG is prohibitively more expensive both in terms of computational cost and

memory requirements. Nevertheless, this reference comments on the inherent difficulties of CG for p-adaptivity compared to DG, see also [16]. Time domain solvers are preferred for their robustness and use parallel explicit DG solvers to increase performance, see for instance [1, 2].

Here, an explicit time domain DG solver is compared to two frequency-domain DG methods, the hybridizable discontinuous Galerkin (HDG) [7–12] and the embedded discontinuous Galerkin (EDG) [13–15] method. Moreover, Section 4 compares the computational aspects of time- and frequency-domain approaches, and a problem of industrial interest is solved in Section 5.

## 2 GOVERNING EQUATIONS

Different sets of equations are used to model aeroacoustic problems, depending of the nature of the underlying mean flow [17]. In the case of rotational mean flow, the linearized Euler or Navier-Stokes equations are used to compute the acoustic near field. The former is solved in this work, both in time and frequency domain, while Section 4.2 gives guidelines when to use the latter.

The time domain 2.5D linearized Euler equations in conservative form are given by

$$\frac{\partial \boldsymbol{q'}}{\partial t} + \boldsymbol{\nabla} \cdot \mathbf{F}(\boldsymbol{q'}) + \mathbf{S}(\boldsymbol{q'}) = \mathbf{f}', \tag{1}$$

where $\boldsymbol{\nabla} := \begin{bmatrix} \dfrac{\partial}{\partial x} & \dfrac{\partial}{\partial r} \end{bmatrix}$, $\boldsymbol{q'} = [\rho'\, u'\, v'\, w'\, p']^T$, $\mathbf{f}'$ is a source term,

$$\mathbf{F}(\boldsymbol{q'}) = \begin{bmatrix} u_0\rho' + \rho_0 u' & v_0\rho' + \rho_0 v' \\ u_0 u' + \dfrac{p'}{\rho_0} & v_0 u' \\ u_0 v' & v_0 v' + \dfrac{p'}{\rho_0} \\ u_0 w' & v_0 w' \\ u_0 p' + \gamma p_0 u' & v_0 p' + \gamma p_0 v' \end{bmatrix}, \text{and}$$

$$\mathbf{S}(\boldsymbol{q'}) = \begin{bmatrix} \rho' \dfrac{v_0}{r} + v' \dfrac{\rho_0}{r} + w' \dfrac{im\rho_0}{r} \\ -u' \dfrac{\partial v_0}{\partial r} + v' \dfrac{\partial u_0}{\partial r} - \dfrac{\rho'}{\rho_0^2} \dfrac{\partial p_0}{\partial x} - p' \dfrac{\partial (1/\rho_0)}{\partial x} \\ -v' \dfrac{\partial u_0}{\partial x} + u' \dfrac{\partial v_0}{\partial x} - \dfrac{\rho'}{\rho_0^2} \dfrac{\partial p_0}{\partial r} - p' \dfrac{\partial (1/\rho_0)}{\partial r} \\ -w' \dfrac{\partial u_0}{\partial x} - w' \dfrac{\partial v_0}{\partial r} + w' \dfrac{v_0}{r} + p' \dfrac{im}{\rho_0 r} \\ (\gamma - 1) \left[ p' \left( \dfrac{\partial u_0}{\partial x} + \dfrac{\partial v_0}{\partial r} \right) - u' \dfrac{\partial p_0}{\partial x} - v' \dfrac{\partial p_0}{\partial r} \right] + \gamma \dfrac{p_0}{r} (v' + imw') + \gamma p' \dfrac{v_0}{r} \end{bmatrix}.$$

In the frequency domain, the response is assumed to be time harmonic. Thus a Fourier decomposition of the form

$$\boldsymbol{q'}(\boldsymbol{x}, t) = \boldsymbol{q}(\boldsymbol{x}; \omega) e^{-i\omega t} \tag{2}$$

is employed, and the main quantities of interest are the acoustic perturbations $\boldsymbol{q}(\boldsymbol{x}; \omega)$ for a given angular frequency $\omega$. By inserting a single mode $\boldsymbol{q}(\boldsymbol{x}; \omega)e^{-i\omega t}$ from the decomposition (2) into (1), and factoring out the term $e^{-i\omega t}$ from both sides of the resulting equation, the obtained system represents the linearized Euler equations in frequency domain

$$-i\omega \boldsymbol{q} + \boldsymbol{\nabla} \cdot \mathbf{F}(\boldsymbol{q}) + \mathbf{S}(\boldsymbol{q}) = \mathbf{f}, \tag{3}$$

with the understanding that the physical response is given by the real part of the solution.

## 3 STATE OF THE ART NUMERICAL METHODS FOR THE LINEARIZED EULER EQUATIONS

This section outlines some aspects of the numerical methods used to solve the LEE in both time and frequency domain.

### 3.1 Time domain

A quadrature-free Runge-Kutta discontinuous Galerkin method (RK-DGM) [18, 19], implemented by the Actran DGM solver, developed by FFT[1], is used for solving the LEE in time domain. This commercial software is designed for predicting the propagation of tonal engine noise components in a moving fluid with shear layers and in the presence of acoustically lined ducts, typically engine nacelle exhausts. It is implemented for unstructured grids in 2D, 2.5D and 3D, employs a fourth order Runge-Kutta temporal scheme and supports variable order of the elements (p-adaptivity). A Godunov first-order upwind method is used to compute the numerical flux on the element interfaces. In order to obtain an upwind scheme for all the characteristic variables, the flux is split into positive and negative components, i.e. waves entering and leaving the element through the corresponding interface, respectively [20]. The mean flow field can be interpolated on the element vertices or on the Gauss points for a more precise sampling. Buffer zones with non-reflecting characteristic boundary conditions are used to minimize spurious reflections from the boundaries. Moreover, planar, cylindrical and spherical sources, as well as incident duct modes and admittance boundaries conditions are also supported.

### 3.2 Frequency domain

The continuous Galerkin (CG) method [21] with appropriate stabilization, has been advocated in [5, 6] for solving the LEE in frequency domain, due to the small computational cost and memory requirements. The discontinuous Galerkin (DG) method [22],

[1]Free Field Technologies S.A - MSC software company.

however, has better dispersive behavior than CG [23], does not require explicit stabilization for convection-dominated problems and is amenable to implement p-adaptivity, but at the same time has more degrees of freedom (DOF). While a comparison with CG is presented in [5], with the conclusion that it is prohibitively more expensive, others [24] compare HDG with CG and indicate different conclusions. Indeed, the HDG [7–12] and the EDG [13–15] methods, retain the aforementioned useful properties of the DG method, and at the same time have very similar (HDG) or same (EDG) number of global DOF as the continuous Galerkin method. The main idea of the HDG method is the hybridization of the unknown variable into a local one on the element, and a global one which lives only on the faces of the elements. The original equations are cast in a local problem, consisting of mapping the local unknowns from the element to the global ones on the faces (similar to *static condensation* in CG), and a global problem which is assembled from all the unknowns on the faces [8–10, 12]. Thus, only the DOF on the faces have contributions to the global system, in this manner reducing the global DOF compared to the compact discontinuous Galerkin (CDG) method [25]. Furthermore, the HDG method has a super-convergence property for second-order elliptic operators after an inexpensive element-by-element post-process [8, 9]. This super-convergence property, however, is not available for the LEE, since they are only first-order. A step further into reducing the node duplication in DG methods has been done with the introduction of the EDG method in [13]. EDG is obtained from the HDG method by changing the space of the global trace unknown from discontinuous to continuous, thus reducing the DOF, and obtaining the same global space and a system with same size and sparsity pattern as the one of the statically condensed CG method. This reduction in the DOF, however, comes at the price of loosing the super-convergence property available with HDG for second order elliptic problems. Moreover, the uniform block structure of the global matrix (which drastically improves computability [24, 26]) is lost, and complications arise for implementing a p-adaptive solution process in 3D. A detail comparison of different Galerkin methods is presented in [27].

## 4 CHALLENGES IN TIME AND FREQUENCY DOMAIN

### 4.1 Computational challenges

**Computational cost.** The cost of an aeroacoustic solver is dominated by the cost to solve the arising global system. Considering that in the frequency domain only a single global system solve is performed, compared to multiple system solves in time domain (until steady-state is reached), solving in frequency domain has significantly smaller computational cost when a solution at discrete frequencies is required.

**Multi-frequency approach.** The higher computational cost of the time domain approach can be somewhat alleviated by inserting multiple frequencies and obtaining a complete broadband solution with a single solve. Accurately modeling and extending impedance boundary condition to multi-frequency time-domain, however, is not trivial

| | HDG | EDG | CDG |
|---|---|---|---|
| **1000** Hz ($h = 0.34, p = 8$) | | | |
| 2D problem | 0.78 GB | 0.58 GB | 4.17 GB |
| 3D problem | 1 074 GB | 490 GB | 2 158 GB |
| **5000** Hz ($h = 0.068, p = 8$) | | | |
| 2D problem | 19 GB | 14 GB | 104 GB |
| 3D problem | 134 352 GB | 61 344 GB | 269 771 GB |

**Table 1**: Memory estimates for HDG, EDG and CDG for a 2D (domain size of $10 \times 10$) and 3D problem (size $10 \times 10 \times 10$), under the assumptions of 8 points per wavelength and the use of an ILU-0 preconditioned iterative solver.

and can introduce additional modeling errors [28, 29]. Additionally, the final time to reach a steady-state for a multi-frequency approach would increase compared to solving for a single frequency, thus augmenting the cost.

**Memory requirements.** Since the solution in the frequency domain is globally coupled, a global system matrix has to be assembled, implying big memory requirements which can become a serious constraint on the problem size. In contrast to this, explicit time-stepping schemes and an element-by-element solution process can be employed for time-domain models, resulting in low memory requirements [1, 30].

The memory requirements in frequency domain when an iterative solver is used can be estimated by $2\mathtt{m}^2\mathtt{nnz} \times 8$ bytes, where `m` is the number of components of the solution (5 in the case of 2.5D LEE), and `nnz` is the number of non-zero entries in the global matrix. If an ILU-0 preconditioner is used, that amount will double. Detailed expressions for the `nnz` of different Galerkin methods can be found in [27]. Typical frequencies of interest, for example for turbofan engine fan noise problem (where the blade pass frequency is around 1 kHz), range from several hundred to several thousand hertz. Table 1 gives the memory estimates for 2D problems of size $10 \times 10$ and 3D problems of size $10 \times 10 \times 10$, for frequencies of 1000 Hz and 5000 Hz, under the assumption of 8 points per wavelength. The estimates show that the memory requirements for the frequency domain solvers in 2D are reasonable. This is also the case for the 3D problem with frequency of 1000 Hz. For medium and high frequencies in 3D, however, the memory requirements are excessive. An explicit time-domain solver should be used for those cases in order to reduce the memory requirements.

### 4.2 Kelvin-Helmholtz instabilities

Kelvin-Helmholtz (KH) instabilities are a physical phenomenon, occurring in the presence of thin shear layers in the flow [17]. When the Navier-Stokes equations are solved, they are limited and modified by non-linear and viscous effects. In the framework of the linearized Euler equations, however, the instabilities are not limited, due to the absence of non-linear and viscous terms in the mathematical model.

A stability criterion has been established by Michalke in [31, 32], stating that instabil-

ities would only appear for Strouhal numbers smaller than a critical value

$$St = \frac{f\theta}{U_j - U_\infty},$$

where $f$ is the frequency, $\theta$ is the momentum thickness of the shear layer, and $U_j$ and $U_\infty$ are the jet and ambient velocities, respectively. This means that for a given mean flow (fixed $\theta, U_j$ and $U_\infty$), the solution would be stable for excitations beyond a critical frequency. For realistic viscous mean flows the instability region would very often be limited to a small portion of the lower part of the spectrum (in the examples considered in this work between $0 - 100\,\text{Hz}$), and it would be outside the range of frequencies one is typically interested in. If that is not the case, however, viscous or non-linear effects have to be considered.

While the frequency $f$ is well defined and constrained (to the excitation frequency) in the frequency domain, this is not the case in the time domain. A time domain solution supports the complete range of frequencies, thus, depending on the problem geometry and mean flow, excitations in the unstable region can appear, and they may trigger the KH instabilities. This renders the instabilities a much bigger problem in time than in frequency domain.

## 5 NUMERICAL EXAMPLES

The problem of acoustic propagation from a duct exhaust is solved in both time and frequency domain in order to compare performance and cross-validate the results. A sketch of the problem is given in Figure 1. The infinite domain is truncated with non-reflecting boundary conditions, symmetric boundary is used on the bottom, and wall boundary conditions ($\boldsymbol{v} \cdot \boldsymbol{n} = 0$) on the duct walls. The incoming wave is imposed by setting source terms in the incoming buffer zone (gray area in Figure 1). Comparisons are made for zero mean flow, and for a realistic mean flow computed with a CFD solver (Fluent).

### 5.1 Duct exhaust with zero mean flow

Pressure maps of the solution for frequencies of 800 Hz and 1282 Hz are given in Figure 2 (top left and right, respectively). A comparison of the sound pressure level (SPL) for the same frequencies computed on the basis of the HDG, EDG and the Actran DGM solutions along the line $y = 3$ is given in Figure 2 (bottom). The SPL is computed as

$$\text{SPL} = 10 \log_{10} \left( \frac{p^2}{p_{ref}^2} \right), \text{ where } p_{ref} = 2 \cdot 10^{-5}\,\text{Pa}. \tag{4}$$

The comparison shows a good match between the solvers, with only minor differences in the case of 800 Hz around $x = 3$, probably due to under-resolution in that region.

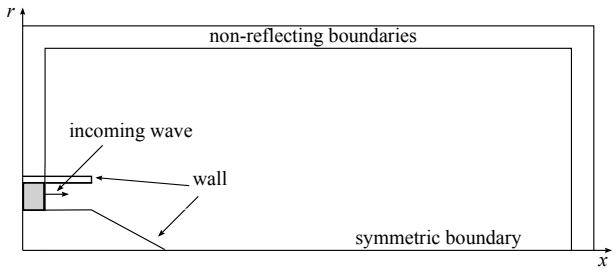


**Figure 1**: Sketch of the duct exhaust problem.

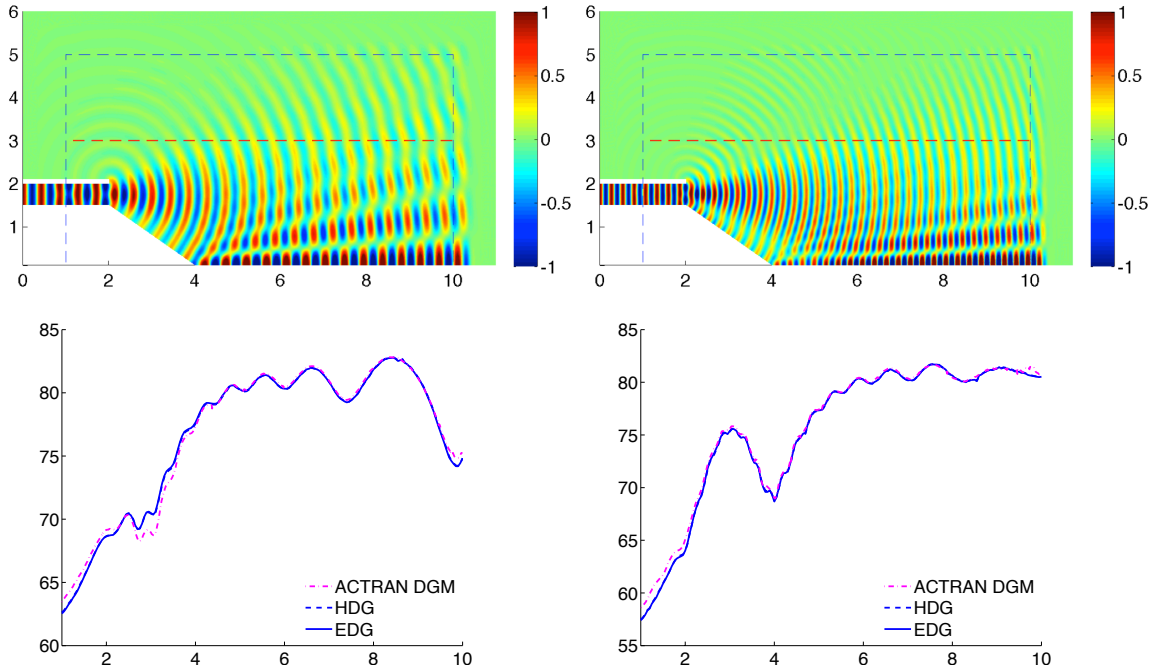


**Figure 2**: Pressure maps of the solutions (top) and sound pressure level (SPL) comparison of HDG, EDG and Actran DGM solutions along the line $y = 3$ (bottom) for frequencies of 800 Hz (left) and 1282 Hz (right).

## 5.2 Duct exhaust with computed mean flow

The mean flow (see Figure 3) is computed with Fluent, it has a velocity magnitude of $M_x = 0.4$ in the duct intake, and the boundary layers are not resolved (free slip boundary condition is used on the walls).

Pressure maps of the solution for frequencies of 800 Hz and 1282 Hz are given in Figure 4 (top left and right, respectively). A comparison of the sound pressure level (SPL) for the same frequencies between the HDG, EDG and Actran DGM solutions along the line $y = 3$ is given in Figure 4 (bottom). The results show good agreement between the solutions for both frequencies, with some expected differences due to the different discretization and

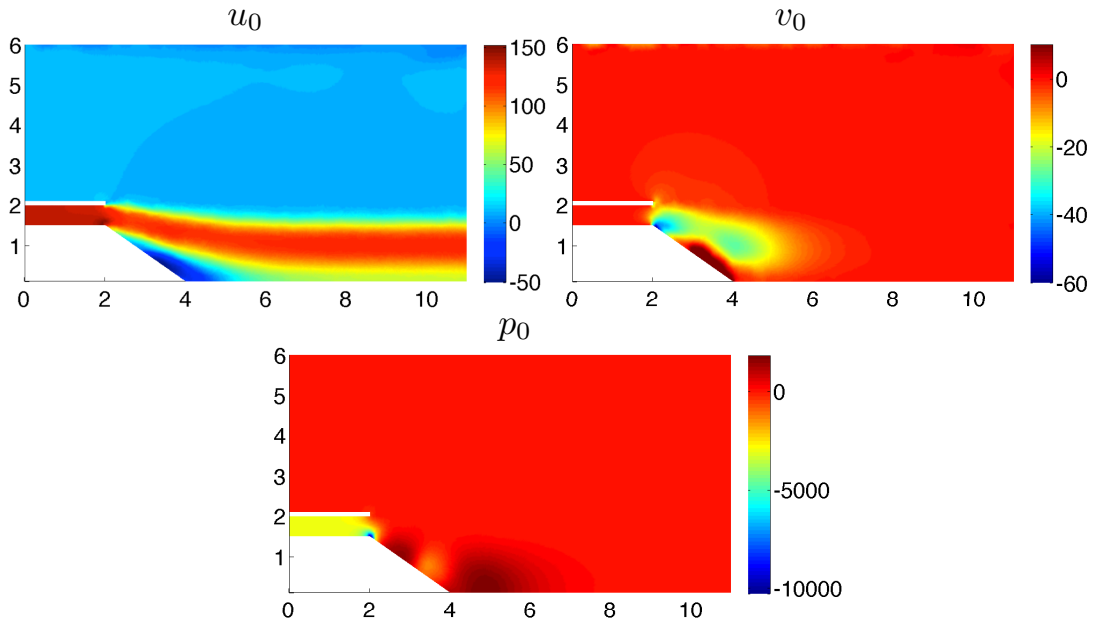


**Figure 3**: Mean flow computed with Fluent.

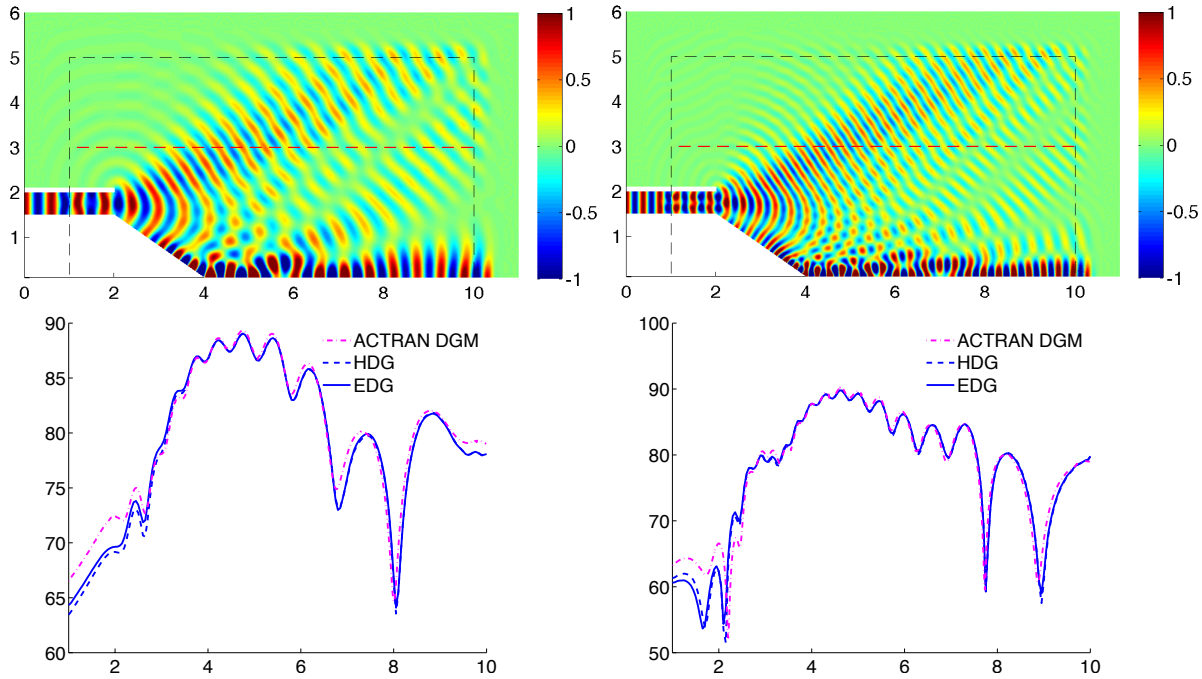


**Figure 4**: Pressure maps of the solutions (top) and sound pressure level (SPL) comparison of HDG, EDG and Actran DGM solution along the line $y = 3$ (bottom) in the presence of mean flow, for frequencies of 800 Hz (left) and 1282 Hz (right).

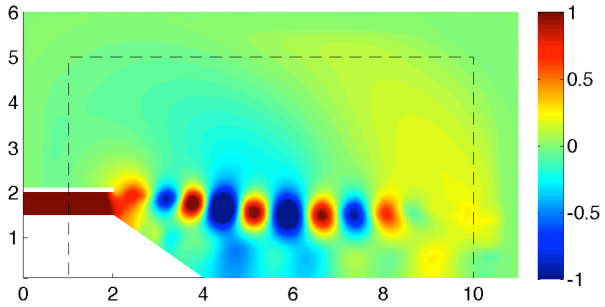


**Figure 5**: Kelvin-Helmholtz instabilities appearing at a frequency of 50 Hz.

| | **Actran DGM** | **HDG** | **EDG** | **CDG** (estimate) |
|---|---|---|---|---|
| **800** Hz | | | | |
| CPU-time | 21' 57" | 3' 4" | 2' 45" | - |
| Peak memory | 143 MB | 615 MB | 454 MB | 1236 MB |
| **1282** Hz | | | | |
| CPU-time | 24' 34" | 4' 33" | 3' 52" | - |
| Peak memory | 154 MB | 1 047 MB | 838 MB | 2920 MB |

**Table 2**: Comparison of CPU-time and peak memory for Actran DGM, HDG, EDG, and a memory estimate for CDG, for frequencies of 800 Hz and 1282 Hz.

sampling of the mean flow.

As noted earlier (Section 4.2), the instability region for this example ranges between $0 - 100$ Hz. The appearance of the KH instabilities for a frequency of 50 Hz is illustrated in Figure 5.

### 5.3 CPU-time and memory requirements

Table 2 gives measurements for CPU-time and peak memory for Actran DGM, HDG, EDG and a memory estimate for CDG. These results clearly state that the HDG and EDG methods in frequency domain reduce significantly the CPU-time compared to the time domain approach, while at the same time reducing the memory requirements compared to the use of CDG in frequency domain. An ILU-0 preconditioned iterative solver (BiCGSTAB, see [33]) has been used to solve the global system. Note that the use of a direct solver would require more memory. The HDG/EDG solution is obtained with constant approximation order in the whole domain. With the implementation of p-adaptivity for the HDG/EDG solver, the total CPU-time and memory requirements could be decreased.

## 6 CONCLUDING REMARKS AND FUTURE WORK

The results and estimates show that while solving the LEE in frequency domain is computationally cheaper, memory requirements can be a bottleneck for high frequencies in 3D

problems with the hardware available today. Total available memory, however, increases faster than computational power, and is easier to harness, making the frequency domain approach more compelling in the medium term even for 3D problems. The HDG and EDG methods reduce significantly the memory requirements of the classical DG, while maintaining its good dispersion and dissipation properties, they evade explicit stabilization and are amenable to p-adaptivity.

Another benefit of the frequency domain approach is the localization of the KH instabilities in a small range of very low frequencies, which typically fall outside the interval of interest. When this is not the case, however, viscous and/or non-linear effects have to be considered, similarly to the time-domain approach, in order to obtain a meaningful solution.

Future work includes the implementation of p-adaptivity for the frequency domain solver, which would reduce both the CPU-time and memory requirements, quantifying the effect of mean flow sampling density and boundary layers on the acoustic perturbation, and considering the viscous effect in order to avoid the KH instabilities in the complete bandwidth.

## REFERENCES

[1] R. Leneveu, B. Schiltz, J. Manera, and S. Caro. Parallel DGM scheme for LEE applied to exhaust and bypass problems. *AIAA Paper 2007-3510. Proceedings of the 13th AIAA/CEAS Aeroacoustics Conference (28th AIAA Aeroacoustics Conference)*, 2007.

[2] R. D. R. Rinaldi, A. Iob, and R. Arina. An efficient discontinuous Galerkin method for aeroacoustic propagation. *Int. J. Numer. Methods Fluids*, 69(9):1473–1495, 2012.

[3] X. Huang, X. Chen, Z. Ma, and X. Zhang. Efficient computation of spinning modal radiation through an engine bypass duct. *AIAA J.*, 46(6):1413–1423, 2008.

[4] Y. Özyörük, E. Alpman, V. Ahuja, and L.N. Long. Frequency-domain prediction of turbofan noise radiation. *J. Sound Vib.*, 270:933 – 950, 2004.

[5] P. Rao and P. Morris. Use of finite element methods in frequency domain aeroacoustics. *AIAA J.*, 44:1643–1652, 2006.

[6] A. Iob, R. Arina, and C. Schipani. Frequency-domain linearized Euler model for turbomachinery noise radiation through engine exhaust. *AIAA J.*, 48:848–858, 2010.

[7] B. Cockburn, B. Dong, and J. Guzmán. A superconvergent LDG-hybridizable Galerkin method for second-order elliptic problems. *Math. Comput.*, 77:1887–1916, 2008.

[8] B. Cockburn, J. Gopalakrishnan, and R. Lazarov. Unified hybridization of discontinuous Galerkin, mixed, and continuous Galerkin methods for second order elliptic problems. *SIAM J. Numer. Anal.*, 47(2):1319–1365, 2009.

[9] N. C. Nguyen, J. Peraire, and B. Cockburn. An implicit high-order hybridizable discontinuous Galerkin method for linear convection-diffusion equations. *J. Comput. Phys.*, 228(9):3232–3254, 2009.

[10] N.C. Nguyen, J. Peraire, and B. Cockburn. A hybridizable discontinuous Galerkin method for Stokes flow. *Comput. Meth. Appl. Mech. Eng.*, 199(9-12):582 – 597, 2010.

[11] N. C. Nguyen, J. Peraire, and B. Cockburn. An implicit high-order hybridizable discontinuous Galerkin method for the incompressible Navier-Stokes equations. *J. Comput. Phys.*, 230(4):1147–1170, 2011.

[12] N. C. Nguyen, J. Peraire, and B. Cockburn. High-order implicit hybridizable discontinuous Galerkin methods for acoustics and elastodynamics. *J. Comput. Phys.*, 230(10):3695–3718, 2011.

[13] S. Güzey, B. Cockburn, and H. K. Stolarski. The embedded discontinuous Galerkin method: application to linear shell problems. *Int. J. Numer. Methods Eng.*, 70(7):757–790, 2007.

[14] B. Cockburn, J. Guzmán, S.-C. Soon, and H. K. Stolarski. An analysis of the embedded discontinuous Galerkin method for second-order elliptic problems. *SIAM J. Numer. Anal.*, 47(4):2686–2707, 2009.

[15] J. Peraire, N. C. Nguyen, and B. Cockburn. An embedded discontinuous Galerkin method for the compressible Euler and Navier-Stokes equations. In *20th AIAA Computational Fluid Dynamics Conference*, volume 2, 2011.

[16] Giorgio Giorgiani, Sonia Fernández-Méndez, and Antonio Huerta. Hybridizable Discontinuous Galerkin p-adaptivity for wave propagation problems. *Int. J. Numer. Methods Fluids*, 72(12):1244–1262, 2013.

[17] R. J. Astley. Numerical methods for noise propagation in moving flows, with application to turbofan engines. *Acoust. Sc. Tech.*, 30(4):227–239, 2009.

[18] N. Chevaugeon, J.F. Remacle, X. Gallez, P. Ploumans, and S. Caro. Efficient discontinuous Galerkin methods for solving acoustic problems. In *Proceedings 11th AIAA/CEAS Aeroacoustics Conference (Monterey CA, USA, May 23-25, 2005) Paper AIAA 2005-2823*, 2005.

[19] N. Chevaugeon, J.F. Remacle, and X. Gallez. Discontinuous Galerkin implementation of the extended Helmholtz resonator impedance model in time domain. In *Proceedings 12th AIAA/CEAS Aeroacoustics Conference (Cambridge MA, USA, May 8-10, 2006), Paper AIAA 2006-2569*, 2006.

[20] Free Field Technologies. *Actran DGM User's manual*. 2014.

[21] P. G. Ciarlet. *The finite element method for elliptic problems*. North-Holland Publishing Co., Amsterdam, 1978. Studies in Mathematics and its Applications, Vol. 4.

[22] B. Cockburn, G. Karniadakis, and C. Shu. *Discontinuous Galerkin Methods: Theory, Computation and Applications*. Springer-Verlag, 2000.

[23] M. Ainsworth. Dispersive and dissipative behaviour of high order discontinuous Galerkin finite element methods. *J. Comput. Phys.*, 198(1):106 – 130, 2004.

[24] Giorgio Giorgiani, David Modesto, Sonia Fernández-Méndez, and Antonio Huerta. High-order continuous and discontinuous Galerkin methods for wave problems. *Int. J. Numer. Methods Fluids*, 73(10):883–903, 2013.

[25] J. Peraire and P.-O. Persson. The compact discontinuous Galerkin (CDG) method for elliptic problems. *SIAM J. Sci. Comput.*, 30(4):25, 2007.

[26] X. Roca, N. C. Nguyen, and J. Peraire. GPU-accelerated sparse matrix-vector product for a hybridizable discontinuous Galerkin method. *49th AIAA Aerospace Sciences Meeting*, pages 1–12, 2011.

[27] A. Huerta, A. Angeloski, X. Roca, and J. Peraire. Efficiency of high-order elements for continuous and discontinuous Galerkin methods. *Int. J. Numer. Methods Eng.*, 96(9):529–560, 2013.

[28] C. Richter, J. Abdel Hay, ł. Panek, N. Schönwald, S. Busse, and F. Thiele. A review of time-domain impedance modelling and applications. *Journal of Sound and Vibration*, 330(16):3859 – 3873, 2011.

[29] S.W. Rienstra. Impedance models in time domain including the extended Helmholtz resonator model. In *Proceedings 12th AIAA/CEAS Aeroacoustics Conference (Cambridge MA, USA, May 8-10, 2006), Paper AIAA 2006-2686*, pages 1–20, 2006.

[30] R. Leneveu, B. Schiltz, S. Laldjee, and S. Caro. Performance of a DGM scheme for LEE and applications to aircraft engine exhaust noise. *14th AIAA/CEAS Aeroacoustics Conference*, 2008.

[31] A. Michalke. On spatially growing disturbances in an inviscid shear layer. *J. Fluid Mech.*, 23:521–544, 1965.

[32] A. Michalke. Survey on jet instability theory. *Prog. Aerosp. Sci.*, 21(0):159 – 199, 1984.

[33] H. A. van der Vorst. BI-CGSTAB: A Fast and Smoothly Converging Variant of BI-CG for the Solution of Nonsymmetric Linear Systems. *SIAM J. Sci. Stat. Comput.*, 13(2):631–644, 1992.